Quantification of Corneal Neovascularization via Contourlet Transform based Segmentation of Blood Vessels

Nesreen.A.Otoum, Eran.A.Edirisinghe

Department Computer Science, Loughborough University, Loughborough, LE11 3TU, UK
N.otoum@lboro.ac.uk, E.A.Edirisinghe@lboro.ac.uk

***Abstract*— This paper proposes a Contourlet Transform based approach to the segmentation of corneal blood vessels that is of clinical importance in the treatment of corneal neovascularisation. The quantification of blood vessels provides means for monitoring the affect of any treatment process being followed. The proposed approach initially uses semi-automated algorithm to detect the corneal area of a high quality colour image of an eye. Subsequently the difference image between the red and green colour planes is subjected to contrast adjustment followed by a novel contrast enhancement algorithm in the Contourlet Transform domain. The enhanced blood vessel images are finally thresholded to form binary images, using which a quantification is carried out based on a measure defined as a ratio of pixels belonging to blood vessels within the area of the cornea. We provide experimental results based on four practical data sets obtained from patients suffering from different levels of corneal neovascularization.**

***Index Terms*— Contourlet Transform, contrast enhancement, corneal neovascularization, segmentation of blood vessels..**

I. Introduction

The normal cornea is devoid of both blood and lymphatic vessels (lymphatic vessels refer to the capillaries, collecting vessels, and trunks that collect lymph from the tissues and carry it to the blood stream).. This avascularity (also termed the *angiogenic privilege of the cornea*) is highly conserved evolutionarily to maintain transparency and visual acuity. Nonetheless, because of a variety of severe inflammatory diseases, the cornea can become invaded by pathologic blood and lymphatic vessels. Pathologic corneal neovascularization (the excessive ingrowth of blood vessels from the limbal vascular plexus into the cornea, i.e., angiogenesis) not only reduces the quality of being able to see objects through the cornea (also called corneal transparency) but also is a major risk factor for corneal transplantation. In addition, host corneal neovascularization— both before as well as after surgery—is one of the most significant risk factors for subsequent immune rejections after replacing the damaged cornea with a clear cornea (corneal grafting). Thus timely and effective treatment of corneal neovascularization is important.

Quantification of corneal neovascularization provides means to monitor the effectiveness of any treatment process. To this affect many corneal imaging devices are capable of providing medical experts with high quality images that may be manually inspected and quantified. However, in severe cases of corneal neovascularization, manual inspection and quantification becomes an extremely tedious, time consuming task prone to human error (figure 1 Illustrates the difference between severe and minor cases in terms of number of the blood vessels growing within the cornea). Automated or semi-automated computer aided inspection and measurement provides a valuable and more accurate alternative approach.

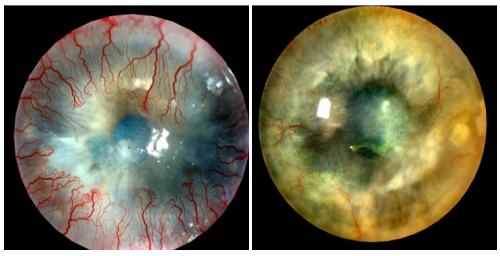

(a) (b)

Fig. 1. Corneal Neovascularization (a) a severe case (b) a minor case.

Literature on the quantification of Corneal Neovascularization focuses more on the clinical analysis aspects and uses basic image processing tools that are implemented within standard imaging applications [1-7]. These include the separation of colour planes, noise removal, contrast adjustment, thresholding based image segmentation etc. The use of these tools requires considerable human intervention and trial and error testing for determining the best threshold values. Further, the segmentation accuracy will depend heavily on the image capture device and varying noise levels. On the other hand some promising approaches have been developed for the enhancement of blood vessels in retinal imaging [8-13]. Our detailed study of using some of the key

techniques adopted in retinal blood vessel enhancement in corneal blood vessel enhancement revealed that the differences of noise levels and the presence of bright reflections and acute variations in background illumination in the latter warrants new approaches to be developed and tested. In this paper we use an approach based on Contourlet Transform [14] which results in a local, flexible multi-resolution and directional image decomposition using contour segments. The directional nature of Countourlet Transforms allows for more accurate representation of contours, allowing their subsequent processing/enhancement to be done more efficiently. Given the fact that corneal blood vessels are of random shapes and orientations and are of varying scale and resolution, the use of Countourlet Transforms in their representation is further justified.

For clarity of presentation this paper is divided into five sections. Apart from section I that introduced the reader to the problem domain and gives an insight to existing solutions, section II presents the proposed approach. Section III provides experimental results and an analysis. Finally section IV concludes with an insight to further possible directions of research.

II. Proposed Approach

A. An Overview

The quantification of corneal neovascularization requires the determination of the ratio between the total area occupied by the blood vessels and the total area of the cornea. This requires both the determination of the boundary of the cornea and the segmentation of all blood vessels.

Although a number of automated corneal area segmentation algorithms have been proposed in literature under the present context of our research which focuses more on the accuracy of segmentation of blood vessels, we decided to use a semi-automatic, accurate, corneal boundary segmentation approach. In this approach an initial elliptically shaped countour is adjusted manually by the user to register with the boundary of the cornea. Although this step requires manual intervention the process is easy and is worth the effort due to the difficulty of automatically detecting the accurate shape of a corneal boundary using any existing image processing approach.

Once the corneal image is segmented it undergoes a number of stages of processing as illustrated by the high level block diagram of figure 2.

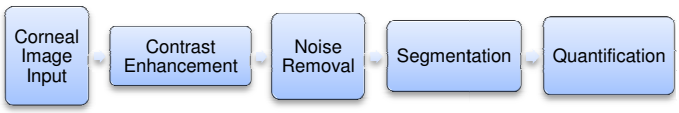

Fig. 2. Proposed approach to corneal neovascularization

The contrast enhancement and noise removal are both done within a Countourlet Transform domain processing procedure described in section II.B. As a result of this stage the contrast of the blood vessels of the corneal image is enhanced. Further noise and non-uniform background illumination is minimized. This allows the simple thresholding based blood vessel extraction algorithm to perform accurately. The final quantification stage quantifies the total area occupied by the blood vessels.

B. Contrast Enhancement and Noise Removal

Figure 3 illustrates a detailed block diagram of the stages involved within this phase of the proposed approach to the quantification of corneal neovascularization. The subsequent sections provide more details of each important sub-stage.

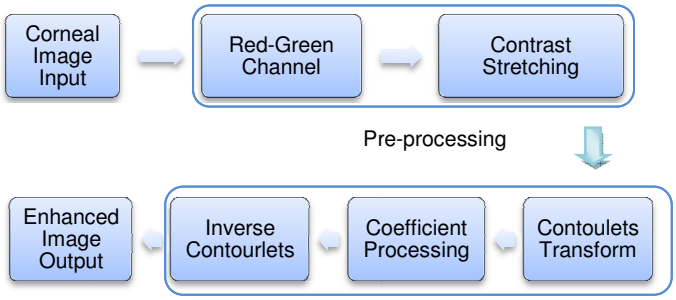

Fig.3. Corneal image enhancement

1) Pre-processing - Removal of non-uniform illumination: The first phase of this stage is the determination of the different images between the red and green colour planes of the original corneal colour image. Our investigations with the three colour planes revealed that either the difference between the red and green plane or the difference between the red and blue planes enables the removal of non-uniform background illumination, which is a major obstacle for the subsequent blood vessel segmentation stages. (see figure 4) Figure 4 (d) illustrates that the highlighted areas have been removed in the difference image between the red and green component images. As we can notice that the highlighted areas have been removed in image (d) the result of difference between the red and green plane.

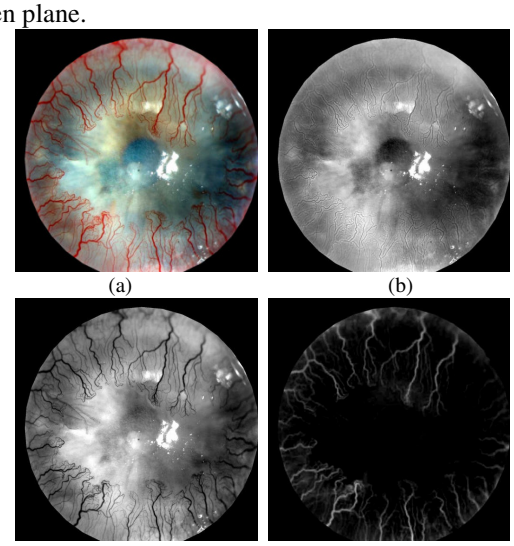

Fig. 4. Removal of non-uniform illumination (a) original colour image (b) red component image (c) green component (d) red-green component image

Subsequent to the formation of the difference image contrast stretching can be used to improve the contrast further. This involves the determination of the highest pixel value and re-mapping it to 255 and the determination of the lowest pixel value and re-mapping it to 0.

2) Contourlet transform: In general the application of Contourlet Transform to an image involves two stages. A Laplacian pyramid is first used to capture point discontinuities followed by the application of a directional filter bank to link point discontinuities into a linear structure (see section II B.4 equation (2) and (3)). The overall result is thus an image expansion using basic elements such as contour segments and is hence named a Contourlet.

Figure 5 illustrates the Contourlet decomposition [14] of a typical corneal image with neovascularization. The specific decomposition illustrated represents a two level decomposition with the first level illustrating four directions and the second level illustrating eight directions. It is noted that blood vessels are represented in their parts within the various sub-bands of decomposition.

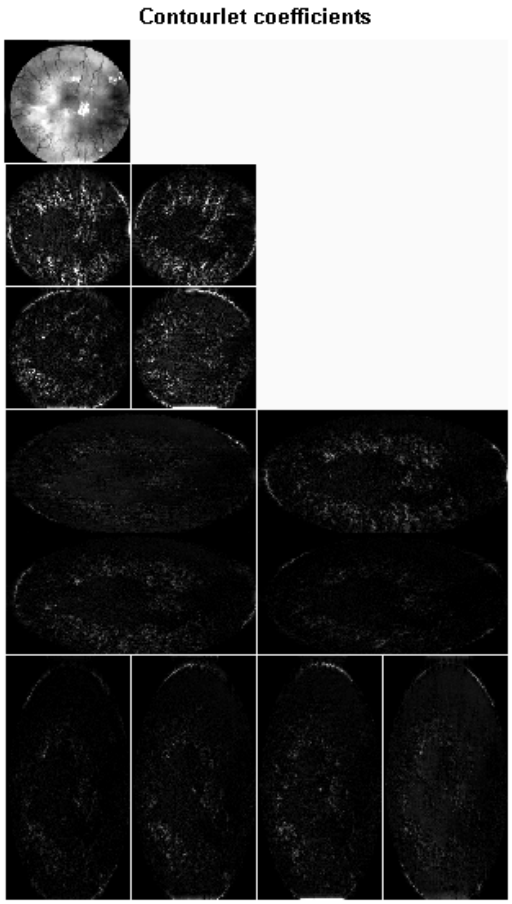

Fig. 5. Two level, 8 band Contourlet decomposition of a corneal image

3) Contourlet based image enhancement: A closer look at the difference image between the red and the green colour plains reveals blood vessels of different luminosity. The vessels having high contrast to the background (bright) are easy to detect but the vessels having low contrast to the background will be more difficult to segment. The approach proposed attempts soften the stronger edges and amplify the faint edges so that the slim vessels will become visible. This is done as follows:

After the decomposition of the image into contourlet coefficients they are modified via a non-linearity function y_α defined below. Note that taking noise into consideration we have adopted a noise standard deviation σ in the equation (see section II B.4).

$$
\begin{aligned}
&y_a(x,\sigma) = 1 && \text{if } x < a\sigma \\
&y_a(x,\sigma) = \frac{x - a\sigma}{a\sigma}\left(\frac{m}{a\sigma}\right)^p + \frac{2a\sigma - x}{a\sigma} && \text{if } a\sigma \le x < 2a\sigma \\
&y_a(x,\sigma) = \left(\frac{m}{x}\right)^p && \text{if } 2a\sigma \le x < m \\
&y_a(x,\sigma) = \left(\frac{m}{x}\right)^s && \text{if } x \ge m
\end{aligned}
\qquad (1)
$$

In the above equations, *m* determines the degree of nonlinearity. *s* introduces dynamic range compression. Using a nonzero *s* will enhance the weaker edges and soften the stronger edges. *a* is a normalization parameter. Parameter *m* is the value under which coefficients are amplified. It is obviously dependent on the values of pixels. There are two possible options to derive the value of *m*,

- $m = K_m\sigma$, which *m* is derived from the noise standard deviation by using parameter K_m. K_m is independent of the Contourlet coefficient values and quite easy for users to set. When *a*=3, K_m=10, all coefficients can be amplified between 3 and 30.
- $m = lM_a$, which *m* is derived from the maximum Contourlet coefficient M_a of the relative sub-band. *l* must be less than 1. In this case, choosing for instance *a*=3 *l*=0.5, we amplify all coefficients with an absolute value between 3σ and half the maximum absolute value of the sub-band.

The first option allows the user to define the coefficients to be amplified as a function of their signal to noise ratio, while the second choice gives a general and easy way to fix the parameter *m* independently of the range of the pixel values.

4) Estimation of noise standard deviation, σ

Estimation of the amount of noise is crucial in many algorithms for digital image analysis. This enables algorithm to adapt to the noise instead of following fixed thresholds. There are a number of standard approaches one can use to estimate the noise variance. Since image structures like edges have strong second order differential components, a noise

estimator should be insensitive to the Laplacian of an image. One of the estimation methods is to suppress the image structure by Laplace masks [15].

The Laplacian of an image *f* can be defined as follows:

$$\nabla^2 f = \frac{\partial^2 f}{\partial x^2} + \frac{\partial^2 f}{\partial y^2} \quad (2)$$

$$\nabla^2 f = f(x+1,y) + f(x-1,y) + f(x,y+1) + f(x,y-1) - 4f(x,y) \quad (3)$$

Immerker in [16] suggests using the difference between two templates L_1 and L_2, approximating the Laplacian of an image in discrete format. The two masks are as follows:

$$L_1 = \begin{bmatrix} 0 & 1 & 0 \\ 1 & -4 & 1 \\ 0 & 1 & 0 \end{bmatrix} \quad L_2 = \frac{1}{2}\begin{bmatrix} 1 & 0 & 1 \\ 0 & -4 & 0 \\ 1 & 0 & 1 \end{bmatrix} \quad (4)$$

The noise estimation operator M is represented by the difference between the two masks above:

$$M = 2(L_2 - L_1) = \begin{bmatrix} 1 & -2 & 1 \\ -2 & 4 & -2 \\ 1 & -2 & 1 \end{bmatrix} \quad (5)$$

which has zero mean and variance $(4^2 + 4 \cdot (-2)^2 + 4 \cdot 1^2)\sigma_n^2 = 36\sigma_n^2$ (6) assuming that the noise at each pixel has a standard deviation σ_n. Assume *f(x, y) * M* denotes the value of applying the mask *M* at position *(x, y)* in the image *f*.

Computing the variance of the output of the *M* operator applied to the image *f,* will give an estimate of $36\sigma_n^2$ at each pixel, which can be averaged over the image *f* or local neighbourhoods to give an estimate of the noise variance σ_n^2. The variance of the noise in *f* can be obtained as,

$$\sigma_n^2 = \frac{1}{36(W-2)(H-2)} \sum_{image\ f} (f(x,y) * M)^2 \quad (7)$$

where *W* and *H* represent the width and height of image *f,* * is the time domain convolution.

To obtain the absolute deviation from the variance above, assuming Gaussian distribution with zero mean and variance σ^2, the deviation is

$$\int_{-\infty}^{\infty} |t| \frac{1}{\sqrt{2\pi}\sigma} \exp\left(\frac{-t^2}{2\sigma^2}\right) dt = \sqrt{\frac{2}{\pi}}\sigma \quad (8)$$

Then,

$$\sigma = \sqrt{\frac{\pi}{2}} \int_{-\infty}^{\infty} |t| \frac{1}{\sqrt{2\pi}\sigma} \exp\left(\frac{-t^2}{2\sigma^2}\right) dt \quad (9)$$

From above, we can obtain σ_n, which is the standard deviation of noise from the variance σ_n^2

$$\sigma_n = \sqrt{\frac{\pi}{2}} \frac{1}{6(W-2)(H-2)} \sum_{image\ f} |f(x,y) * M| \quad (10)$$

5) Inverse Contourlet transform: Once the coefficients have been modified following the above procedure the inverse contourlet transform is used to obtain the enhanced image. Figure 6 illustrates a typical example.

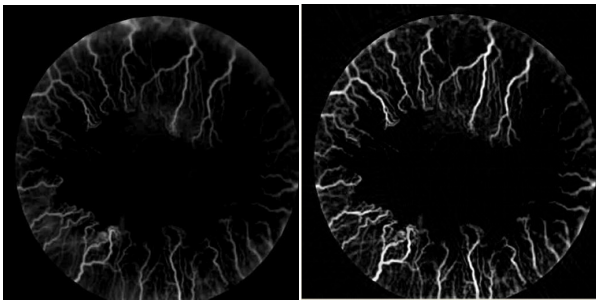

(a) (b)

Fig. 6. The difference between the red and green component images (a) before application (b) after application, of countourlet based enhancement.

6) Contrast enhancement filter: The following 2-D filter was applied on the output of the previous step (Inverse contourlet transform)

$$\frac{1}{(a+1)}\begin{bmatrix} -a & a-1 & -a \\ a-1 & a+5 & a-1 \\ -a & a-1 & -a \end{bmatrix} \quad (11)$$

C. Segmentation

After the images have been enhanced following the procedure described in II.B we use a simple threholding based approach to segment the blood vessels (Note – experimental selection of threshold that results in the best perceptual results). In doing so we create a binary image with 0 (black) representing pixel values outside the blood vessels and 255 (white) representing pixel values belonging to the blood vessels.

Figure 7 illustrates the resulting blood vessel segmentation obtained by following the contrast enhancement procedure described in II.B

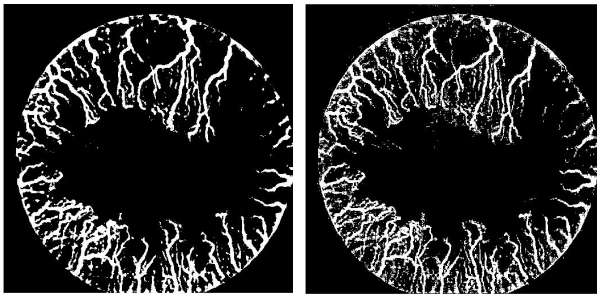

(a) (b)

Fig. 7. The segmentation result (a) before application (b) after application, of Contrast enhancement filter.

D. Thinning.

We applied a standard Thinning approach to make the blood vessels more analogous to the ones on the original image.

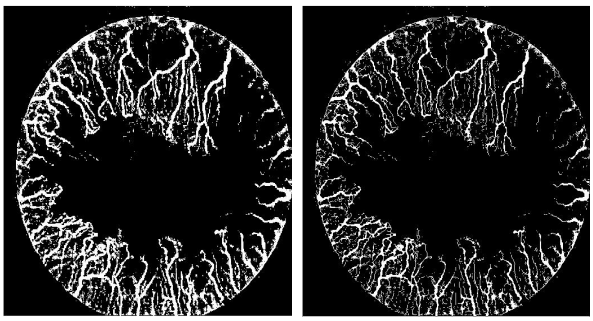

(a) (b)

Fig. 8. The segmentation result (a) before application (b) after application, of the Thinning algorithm.

E. Quantification

For each image the total amount of pixels belonging to the entire corneal area and the total amount of pixels belonging to the blood vessels are calculated.

III. Experimental Results & Analysis

Experiments were performed on a set of four images with various degrees of corneal neovascularisation. All algorithms were implemented with Maltab. The results are illustrated in Figures 9. The images in figure 9 have been arranged in descending order of the degree of corneal neovascularization. The results illustrates the capability of the proposed approach to enhance the blood vessels before segmentation, making the quantifications more accurate.

Table-1 tabulates the quantification results for four test images.

Table.1 Quantification results

	Threshold	Cornea area	Vessel area	Ratio%
Image 1	35	196022	72491	36.9
Image 2	35	197199	51138	25.9
Image 3	70	186190	42728	22.9
Image 4	135	157139	13374	8.5

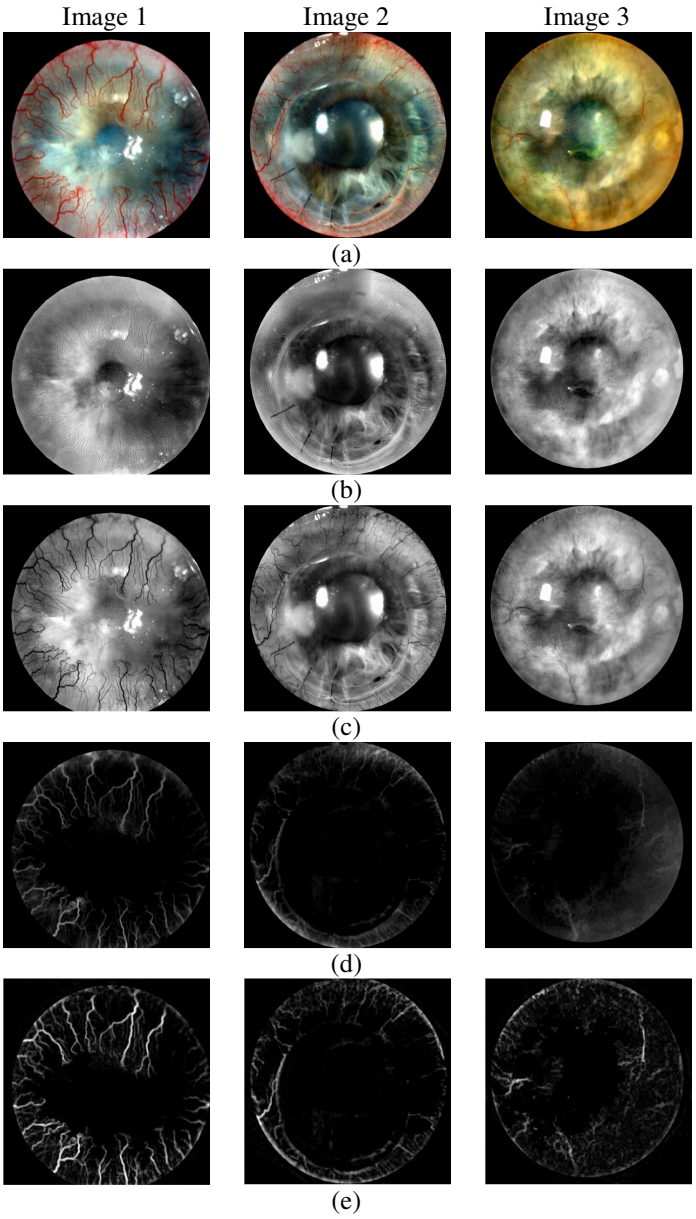

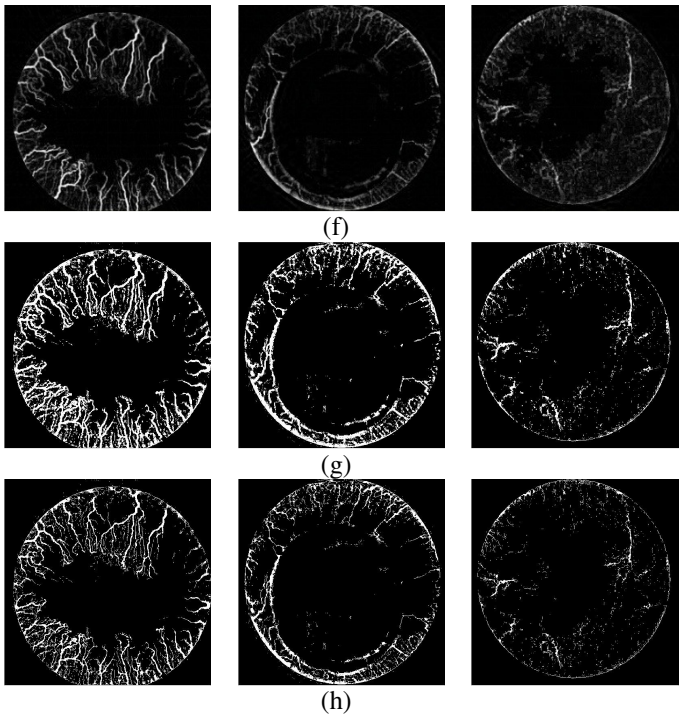

Fig. 9. Experimental Results (a) original colour images (b) red component images (c) green component images (d) The difference between the red and green component image, before enhancement (e) The difference between the red and green component image after countoulet based enhancement (f) result after applying the contrast enhancement filter (g) binary images after segmentation that was used in the quantification.(h) Result after the Thinning algorithm is applied

A closer investigation of the test image (2) of figure 9 illustrates that the proposed approach is also able to remove the consideration of suture marks that are present in the original image due to surgical intervention. Further, the approach has been able to perform remarkably well in the presence of significant effects of non-uniform illumination and reflections.

IV. CONCLUSIONS

We have proposed an efficient computer aided approach to the quantification of corneal neovascularization. The approach is based on the use of Contourlet Transforms to enhance the blood vessels before their segmentation is carried out. A special feature of the approach is that it is robust to different levels of noise that may be present in corneal images. We have shown that the proposed approach is capable of performing effectively in the presence of noise, non-uniform illumination and reflections. Quantifications experiments were done on four corneal images and the performance of the algorithms were analysed at various stages.

At present we are working on making the proposed approach fully automated by introducing an efficient and

robust approach to the determination of corneal boundary and the determination of threholding values used in the final stage of segmentation.

ACKNOWLEDGMENT

The authors would like to extend their gratitude to Prof. H. Duaand Ms L.Faraj, Queens Medical Centre, Nottingham University, UK for their support and advice.

REFERENCES

[1] F.Scarpa,E. Grisan and A.Ruggeri" Automatic Recognition of Corneal Nerve Structures in Images from Confocal Microscopy", Investigative Ophthalmology & Visual Science, November 2008, Vol. 49, No. 11.

[2] F. Bock, J. Onderka, D. Hos, F. Horn, P. Martus, C. Cursiefen "Improved semiautomatic method for morphometry of angiogenesis and lymphangiogenesis in corneal flatmounts" Elsevier, Experimental Eye Research, 2008 ,87,pp.462–70.

[3] C.Cursiefen, F.Bock, F.Horn, F. Kruse, et. "GS-101 Antisense Oligonucleotide Eye Drops Inhibit Corneal Neovascularization" American Academy of Ophthalmology, September 2009, Vol. 116, No. 9.

[4] Proia AD, Chandler DB, Haynes WL,." Quantitation of corneal neovascularization using computerized image analysis" Lab Invest. 1988 Apr,58(4):473-9.

[5] M.Dabbaha, J. Grahama, M.Tavakolib, et. "Nerve Fibre Extraction in Confocal Corneal Microscopy Images for Human Diabetic Neuropathy Detection using Gabor Filters", JDRF scholar grant 17-2008-1031.

[6] Cursiefen C, Wenkel H, Martus P, et. "Standardized semiquantitative analysis of corneal neovascularization using projected corneal photographs--pilot study after perforating corneal keratoplasty before immune reaction". Klin Monbl Augenheilkd. 2001 Jul,218(7),484-91.

[7] I.Bahar, I.Kaiserman, P.McAllum, D.Rootman, and A.Slomovic "Subconjunctival Bevacizumab Injection for Corneal Neovascularization" Lippincott Williams & Wilkins, February 2008,Vol. 27, No 2.

[8] B. S.Yan Lam and H. Yan, "A Novel Vessel Segmentation Algorithm for Pathological Retina Images Based on the Divergence of Vector Fields" IEEE TRANSACTIONS ON MEDICAL IMAGING, FEBRUARY 2008, VOL. 27, NO. 2,

[9] Q.Li, J.You, L.Zhang.et. "Automated Retinal Vessel Segmentation Using Multiscale Analysis and Adaptive Thresholding" IEEE 2006 1-4244-0069-4/06.

[10] L. Espona, M. Carreira, M. Penedo, et." Retinal Vessel Tree Segmentation using a Deformable Contour Model" , IEEE 2008 978-1-4244-2175-6/08.

[11] P.Feng, Y.Pan, B.Wei,et. "Enhancing retinal image by the Contourlet transform" , Pattern Recognition Letters 28 (2007) 516–522 .

[12] A.C Shore "Capillaroscopy and the measurement of capillary pressure". Blackwell Science 2000, 50(6), 501–513.

[13] Hern S, Mortimer PS." Visualization of dermal blood vessels--capillaroscopy.", Clin Exp Dermatol. 1999 Nov;24(6):473-8.

[14] M.N.Do, M.Vetterli, The Contourlet transform: an efficient directional multiresolution image representation, IEEE Trans. On Image Processing, 14(12), pp 2091-2106, 2005.

[15] Zhen-bing Zhao, Jin-sha Yuan, Qinag Gao, Ying-hui Kong. Wavelet Image De-noising Method Based on Noise Standard Deviation Estimation. Proceeding of the 2007 International Conference on Wavelet Analysis and Pattern Recognition, Beijing, China, 2-4 Now. 2007

[16] John Immerker. Fast Noise Variance Estimation. Computer Vision and Image Understanding Vol. 64, No.2, September, pp. 300-302, 1996 ARTICLE NO. 0060